Nitroxide spin exchange due to re-encounter collisions in a series of *n*-alkanes

Mark R. Kurban,[a] Miroslav Peric, and Barney L. Bales
Department of Physics and Astronomy and The Center for Supramolecular Studies, California State University at Northridge, Northridge, California 91330, USA

(Received 19 February 2008; accepted 25 June 2008; published online 8 August 2008)

Bimolecular collisions between perdeuterated 2,2,6,6-tetramethyl-4-oxopiperidine-l-oxyl molecules in three alkanes have been studied by measuring the electron paramagnetic resonance (EPR) spectral changes induced by spin exchange. We define an "encounter" to be a first-time collision followed by a series of re-encounters prior to the diffusing pair's escaping each other's presence. The present work stems from a recent proposal [B. L. Bales *et al.*, J. Phys. Chem. A **107**, 9086 (2003)] that an unexpected linear dependence of the spin-exchange-induced EPR line shifts on spin-exchange frequency can be explained by re-encounters of the same probe pair during one encounter. By employing nonlinear least-squares fitting, full use of the information available from the spectral changes allows us to study encounters and re-encounters separately. The encounter rate constants appear to be dominated by hydrodynamic forces, forming a common curve for hexane, decane, and hexadecane when plotted against T/η, where η is the shear viscosity. Unexpectedly, encounters are not dependent on the ratio $\mu=a/a_s$, where a and a_s are the van der Waals radii of the nitroxide probe and the solvent, respectively. It is argued that the near coincidence of the resulting encounter rate constant with the hydrodynamic prediction is likely due to a near cancellation of terms in the general diffusion coefficient. Thus, the semblance of hydrodynamic behavior is coincidental rather than intrinsic. In contrast, the mean times between re-encounters do depend on the relative sizes of probe and solvent. For hexane at lower temperatures, the Stokes–Einstein equation apparently describes re-encounters well; however, at higher temperatures and for decane and hexadecane, departures from the hydrodynamic prediction become larger as μ becomes smaller. This is in qualitative agreement with the theory of microscopic diffusion of Hynes *et al.* [J. Chem. Phys. **70**, 1456 (1979)]. These departures are well correlated with the free volume available in the solvent; thus, the mean times between re-encounters form a common curve when plotted versus the free volume. Because free volume is manifested macroscopically by the isothermal compressibility, it is expected and observed that the re-encounter rate also forms a common curve across all three solvents when plotted with respect to compressibility. The existence of a common curve for alkanes raises the prospect of using EPR to determine the compressibility of substances such as fossil fuels and biological membranes. © *2008 American Institute of Physics*. [DOI: 10.1063/1.2958922]

I. INTRODUCTION

A great deal of research, both theoretical and experimental, has been devoted to those aspects of electron paramagnetic resonance (EPR) involving Heisenberg spin exchange and its relationship to molecular translational and rotational diffusion in liquids.[1–19] Summarizing a great deal of work, a monograph[4] published in English in 1980 gathered a wealth of theoretical and experimental data and described the use of the spin-exchange technique to study problems in chemistry and biology. In a collision involving two radicals, the quantum mechanical probability for spin exchange is associated with an overlap of the orbitals of unpaired electrons on two probes. This probability is characterized by the exchange integral $J(r)$, which is a rapidly varying function of the distance of approach r between the two probe molecules. Assuming sudden collisions, in which J is switched on for a time τ_c while the two orbitals overlap, the spin-exchange frequency, ω_e, may be written as follows:[8]

$$\omega_e = \tau_E^{-1} f \frac{J^2\tau_c^2}{1+J^2\tau_c^2}, \tag{1}$$

where τ_E is the mean time between encounters of the spin probes and $f=\frac{1}{2}$ for nitroxide spin probes.[4] Strong exchange, $J^2\tau_c^2 \gg 1$, has been invariably found[4] for uncharged nitroxide probes yielding $\tau_E^{-1}=2\omega_e$ from Eq. (1). Thus, τ_E^{-1} may be determined directly by measuring ω_e. The vast majority of studies in the literature have used line broadening to measure ω_e, but recently line shifts and a spin-exchange-induced "dispersion" have been shown to yield rather precise values in some circumstances.[20–22]

Most research in this area has assumed that the spin-exchange encounter between two probes involves a single collision event whereby the pair meets and parts ways without spending a subsequent interval of time together in the

[a]Author to whom correspondence should be addressed. Electronic mail: mark.kurban.75@csun.edu.

TABLE I. van der Waals sizes of solvent molecules and fits to Eq. (17).

Solvent	a_s (Å)	μ	B_{RE}[a]	r[b]	B_E[c]	r[b]
Hexane	3.0	1.2	−1.37	0.995	−0.59	0.999
Decane	3.5	1.0	−1.29	0.968	−0.73	0.999
Hexadecane	4.1	0.86	−1.16	0.972	−0.82	0.999

[a]Re-encounters.
[b]Coefficient of correlation.
[c]Encounters.

same local equilibrium region. Nevertheless, it is well known that bimolecular encounters in liquids are not generally that simple. The concept of a "cage" evolved[23] due to the work of Noyes[24] and others,[25,26] within which two molecules recollide a number of times before finally diffusing apart on the way to another encounter. We have adopted the term "encounter" to mean a first-time collision followed by a series of re-encounters. Thus, an encounter may involve repeated Heisenberg spin exchanges.

The present work was motivated by a recent proposal[22] that an anomalous line shift dependence on ω_e was due to the occurrence of spin exchange during re-encounters. To test that proposal, we have carried out spin-exchange measurements of the small nearly spherical spin probe perdeuterated 2,2,6,6-tetramethyl-4-oxopiperidine-l-oxyl (PDT) in a series of *n*-alkanes. Because *n*-alkanes are known to interact with a solute relatively weakly, they are quite often used as model systems to test theories of diffusion and the predictions of molecular dynamics calculations.[27] It was anticipated that the re-encounter rate, being dominated by a local solvent structure, ought to depend on the relative size of the probe and solvent molecules, $\mu=a/a_s$, where a and a_s are the radii of the probe and solvent molecules, respectively. PDT has a radius of $a=3.5$ Å. The solvents chosen were hexane ($a_s=3.0$ Å), decane ($a_s=3.5$ Å), and hexadecane ($a_s=4.1$ Å), yielding $\mu=1.2$, 1.0, and 0.86, respectively (Table I). These values fall within a region in which substantial departures from hydrodynamic behavior are expected. The main purposes of this work are (1) to add further support for the proposal that re-encounter rates can be measured, (2) to gain insight into the similarities and differences between encounters and re-encounters, and (3) to relate encounters and re-encounters to solvent properties.

II. THEORY

The effect of re-encounters between spin probes on spectra influenced by spin exchange had been neglected in all experimental work until recently,[22] principally because there seemed to be a good agreement with theory without taking them into account.[4] Recently, however, improved precision in data collection and least-squares fitting methods have uncovered a significant discrepancy in the predicted line shifts.[21,22,28,29] The theoretical contributions of re-encounters to spin-exchange spectra derived by Salikhov[31] have brought experiment and theory into agreement for strong exchange conditions and have allowed the measurement of τ_{RE}^{-1}.[22]

The encounter time may be approximated from

$$\tau_E^{-1} = [\text{probe}]K_E, \tag{2}$$

where [probe] is the probe concentration and K_E is the Smoluchowski encounter rate constant given by[4]

$$K_E = 4\pi b D_M, \tag{3}$$

with $D_M=2D$ being the sum of each self-diffusion coefficient D of the two probes and b the distance of bimolecular approach at which collision occurs.

The shape $Y'(H,\omega_e)$ of the first-derivative spectrum for a nitroxide radical is given by[22]

$$Y'(H,\omega_e) = \sum_{M_I} [A_{M_I}{}^S Y'_{A,M_I}(H) + V_{\text{disp}}(M_I) D'_{M_I}(H)], \tag{4}$$

where ${}^S Y'_{A,M_I}(H)$ is the Lorentzian–Gaussian sum function for line M_I given by Eq. (13) of Ref. 30 and A_{M_I} is the doubly integrated intensity of that line. The sum function is an excellent approximation to the Voigt line shape that describes inhomogeneously broadened spin probe spectra.[22] The second term in Eq. (4) is the spin-exchange-induced dispersion derived for nitroxide spin probes[20] from perturbation theory[4] having the property that $V_{\text{disp}}(M_I)=-V_{\text{disp}}(-M_I)$. The sum in Eq. (4) is over all values of the nuclear spin quantum number M_I (1, 0, and −1 for ^{14}N), with H representing the magnetic field, $V_{\text{disp}}(M_I)$ the spin-exchange dispersion height, and $D'_{M_I}(H)$ the first derivative of the spin-exchange dispersion line given by Eq. (10) of Ref. 21. Accurate values of the Lorentzian linewidths may be deduced from the overall linewidth $\Delta H^0_{\text{p.p.}}(M_I)$ by employing the mixing parameter η_{M_I}.[30] Other spectral parameters, including A_{M_I}, may also be determined (see Ref. 22 for full details). Values of the peak-to-peak line height $V_{\text{p.p.}}(M_I)$ are calculated as follows:[30]

$$V_{\text{p.p.}}(M_I) = \frac{A_{M_I}}{\Delta H^0_{\text{p.p.}}(M_I)^2}\left[\eta_{M_I}\frac{\sqrt{3}}{\pi} + (1-\eta_{M_I})\frac{8}{\sqrt{2\pi e}}\right]$$

$$= \frac{A_{M_I}}{\Delta H^0_{\text{p.p.}}(M_I)^2}(1.936 - 1.384\eta_{M_I}). \tag{5}$$

We have improved our software to fit the parameters of Eq. (4), allowing a seamless transition from inhomogeneously broadened lines to Lorentzian line shapes characteristic of higher spin exchange frequencies. This avoids the extra work involved in separately fitting spectra at low and high values of ω_e, as was necessary previously. In the absence of re-encounters, ω_e may be deduced from the EPR spectrum from line broadening, line shifts, or $V_{\text{disp}}(M_I)$.

The broadening B_{M_I} of the M_I hyperfine line is defined as

$$B_{M_I} = \Delta H^L_{\text{p.p.}}(\omega_e)_{M_I} - \Delta H^L_{\text{p.p.}}(0)_{M_I}, \tag{6}$$

with $\Delta H^L_{\text{p.p.}}(\omega_e)_{M_I}$ denoting the peak-to-peak width of the first derivative of the Lorentzian line at a given spin-exchange frequency ω_e, and $\Delta H^L_{\text{p.p.}}(0)_{M_I}$ the corresponding width at zero spin exchange. From the average broadening, ω_e may be obtained as follows:[21]

$$\omega_e = \frac{3\sqrt{3}\gamma\langle B\rangle}{4}, \tag{7}$$

where γ is the gyromagnetic ratio of the electron and $\langle B\rangle$ is the average broadening for all three lines,

$$\langle B\rangle = \tfrac{1}{3}(B_{+1} + B_0 + B_{-1}). \tag{8}$$

The corresponding dispersion-based value for the spin exchange of the nitroxide radical is given by

$$\omega_e = \frac{3\sqrt{3}\gamma A_0}{4|M_I|}\frac{V_{\mathrm{disp}}(M_I)}{V_{\mathrm{p.p.}}(M_I)}\left[1 - \sqrt{2}\left(\frac{V_{\mathrm{disp}}(M_I)}{V_{\mathrm{p.p.}}(M_I)}\right)^2\right], \tag{9}$$

where A_0 is the intrinsic hyperfine separation at zero spin exchange. The leading term of Eq. (9) is predicted by perturbation theory,[20] while the correction term is described in the Supporting Information.[32]

In the theory neglecting re-encounters, the spin-exchange frequency is also predicted implicitly through Eq. (7) from the line shifts as follows:[20]

$$\frac{A_{\mathrm{abs}}}{A_0} = 1 - \frac{9}{32}\left(\frac{\langle B\rangle}{A_0}\right)^2, \tag{10a}$$

where A_{abs} is one-half the difference in resonance fields of the high- and low-field absorption components of the EPR spectrum. It has been shown[22,31] that when probe re-encounters are taken into account, an additional term linear in $\langle B\rangle$ enters the relation:

$$\frac{A_{\mathrm{abs}}}{A_0} = 1 - \kappa\frac{\langle B\rangle}{A_0} - \frac{9}{32}\left(\frac{\langle B\rangle}{A_0}\right)^2, \tag{10b}$$

where

$$\kappa = \frac{\sqrt{3}}{8}(1+\sqrt{2})\sqrt{\frac{\gamma A_0 \tau_{\mathrm{RE}}}{2}}, \tag{11}$$

where τ_{RE} is the mean time between re-encounters. With Eq. (10b) it becomes necessary to obtain independent values for both the broadening and line shift, as the linear term $\kappa(\langle B\rangle/A_0)$ introduces a third variable. An independent determination of the broadening and hyperfine separation and fitting of the coefficient κ in Eq. (10b) to the experimental results lead to a value of τ_{RE} through Eq. (11).

The Stokes–Einstein–Smoluchowski equation for a spherical particle of radius a results from substituting the Stokes–Einstein (SE) equation for the diffusion coefficient of one probe,

$$D = \frac{kT}{6\pi a\eta}, \tag{12}$$

into Eq. (2), yielding, after converting to units L/mol s

$$K_E = \frac{8RT}{3000\eta} = 2K_e, \tag{13}$$

with K_e representing the spin-exchange rate constant. In Eq. (13), use is made of the fact that the two colliding probes are of equal size and the collision distance b is assumed to be equal to $2a$. The van der Waals radius $a=3.5$ Å for PDT is derived using the improved[33] method of Bondi[34] and is also obtained experimentally.[35] The second equality in Eq. (13) expresses the fact that for two nitroxide probes, the spin-exchange rate constant is equal to one-half the rate constant for encounters.[4]

The re-encounter time employing the continuous diffusion model is given by[31]

$$\tau_{\mathrm{RE}} = \frac{b^2}{2D}, \tag{14a}$$

which, in the Stokes–Einstein approximation [Eq. (12)], becomes

$$\tau_{\mathrm{RE}} = \frac{3\pi b^3\eta}{2kT}. \tag{14b}$$

We assume the collision distance b to be the same for encounter and re-encounter spin exchanges because the exchange integral depends principally on separation distance and not on diffusive properties of the environment.

Classical hydrodynamic theory assumes a continuous, nondiscrete medium and holds therefore in the limit of a high probe-to-solvent volume ratio. An important adjustment to hydrodynamic theory is the recognition that a solvent is not a continuous medium but that cavities exist between solvent molecules. One of the early mathematical treatments of intermolecular cavities in liquids was advanced by Frenkel.[36] Recognizing the fact that in a state of maximal compression, a substance will still possess free spaces between its molecules, the total compressible free volume V_f is defined as

$$V_f = V - V_0, \tag{15}$$

where V and V_0 are the total volumes of the sample at T and $T=0$ K.

An empirically based model for free volume was developed by Doolittle,[37] specifically within the context of n-alkanes. His analysis of precisely and accurately measured alkane densities found that

$$V_f/V_0 = e^{((\alpha-10)/M+\beta)} - 1, \tag{16a}$$

where M is the molecular weight and the parameters α and β were dependent on temperature according to

$$\alpha = e^{0.002\,75T+2.303} \tag{16b}$$

and

$$\beta = 0.000\,182T^{1.19}. \tag{16c}$$

Extrapolation to absolute zero temperature yields $\alpha=10$ and $\beta=0$, yielding $V_f=0$.

Doolittle also found empirically that the viscosity of alkanes could be represented satisfactorily as an exponential function of fractional free volume.[37] Using simple theoretical considerations, Cohen and Turnbull were able to derive a similar functional dependence between the diffusion constant D and the free volume V_f.[38] According to the Doolittle–Cohen–Turnbull free volume equation,[37–39]

$$D = A_{\mathrm{FV}}e^{-B(V_0/V_f)}, \tag{17}$$

where A_{FV} and B are constants for a given solute-solvent system. B is the product of a free volume overlapping factor

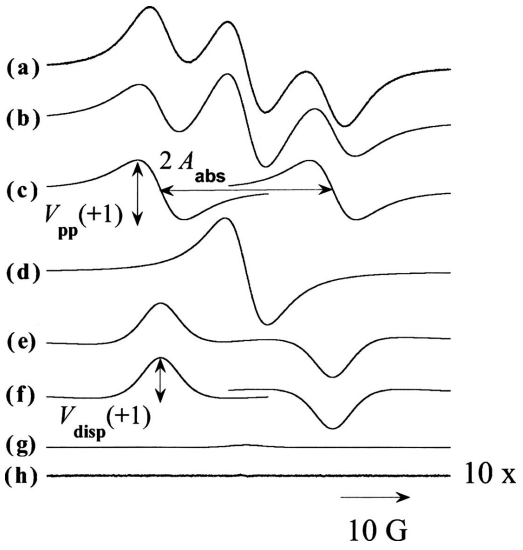

FIG. 1. (a) Experimental spin-exchange-broadened EPR spectrum of 40 mM perdeuterated Tempone in hexadecane at 323 K. The experimental spectrum and the best fit to it are almost perfectly matched. (b) The absorption component of the fit. (c) The outer absorption lines corresponding to nuclear spins +1 and −1, the distance between which is twice the hyperfine coupling spacing. (d) The central absorption line ($M=0$). (e) The dispersion component of the fit. (f) The $M=+1$ and $M=-1$ dispersion lines shown individually. (g) The instrumental dispersion, which is subtracted from the dispersions of the outer lines. (h) The difference between the experimental spectrum and the fit.

$\gamma(0.5 \leqslant \gamma \leqslant 1)$ and the ratio ν^*/V_0, where ν^* is a critical free volume just large enough for a probe molecule to diffuse into it. Because both re-encounter rates and spin-exchange rate constants are proportional to the diffusion coefficient, both are predicted to vary as $e^{-B(V_0/V_f)}$.

III. MATERIALS AND METHODS

The probe employed was 97% PDT purchased from CDN Isotopes. This was dissolved in the following solvents: 99% *n*-hexadecane and 99+% *n*-decane obtained from Sigma-Aldrich and 99+% *n*-hexane produced by MCB Reagents. For each solvent, a mother solution was prepared at a concentration near the saturation point and then vortexed for 24 h. The mother solution was then successively diluted by weight to yield solutions with lower concentrations. From each solution, a sample was extracted into open-ended polytetrafluoroethylene (PTFE) tubing manufactured by Zeus. The tubing was then folded in half to form a vee and the open ends were sealed using an open flame and pliers. The sealed PTFE tubing was then placed, folded end down, into a quartz tube made by Wilmad Glass Co. that had a hole at the bottom, and the quartz tube was then inserted into the cavity of a Bruker ESP 300E spectrometer. Nitrogen gas used to control the temperature flowed past the sample in the cavity prior to the start of measurement in order to purge it of the oxygen that is known to cause excess broadening of the EPR lines.[40] The amount of time spent on removal of oxygen was 30 min for hexadecane and 60 min for decane and hexane.

Spectral measurements of the sample were performed using a sweep width of 60 G, modulation amplitude of 0.2 G, sweep time of 41.94 s, and microwave power of 5.02 mW. The temperature of the sample was monitored with a thermocouple manufactured by Bailey Instruments. Five spectra were taken at each temperature with intervals of 10 K between temperatures. Measurement temperatures were kept constant within ±0.2 K.

IV. RESULTS

Figure 1(a) shows an experimental EPR spectrum of 40 mM PDT in hexadecane at 323 K and its fit. Spectral fits were achieved, as previously described in Ref. 22. The difference between the spectrum and its fit to Eq. (4) is given in Fig. 1(h) showing that the fit is excellent. The absorption component of the best fit is shown in Fig. 1(b) and the dispersion component in Fig. 1(e). To illustrate the experimental fitting procedure used in this work and to define some of the extracted quantities, the fitted absorption spectrum from Fig. 1(b) is split into three individual EPR lines shown in Figs. 1(c) and 1(d). The fitted individual dispersion EPR lines are presented in Figs. 1(f) and 1(g).

It has long been known that EPR spectra can be influenced by instrumental dispersion introduced by an improperly tuned microwave bridge. The instrumental dispersion is barely evident in the central line [Fig. 1(g)] where spin-exchange-induced dispersion is not manifest. The values of spin-exchange-induced dispersion are corrected for instrumental dispersion by subtracting values of $V_{\mathrm{disp}}/V_{\mathrm{p.p.}}$ observed in the central line from the outer lines.

Figure 1(c) defines the hyperfine spacing that is employed in Eqs. (10a), (10b), and (11) and $V_{\mathrm{p.p.}}$, used in Eq. (9), while Fig. 1(f) defines V_{disp}. Note that these parameters can be measured only by fitting the experimental spectrum, so the information contained in these parameters cannot be acquired from simple measurements on the EPR spectrum. In particular, note that A_{abs} is *not* one-half the spacing of the lines in Fig. 1(a); the outer lines in Fig. 1(c) must be used.

Spin-exchange frequencies for each temperature were computed from line broadening through Eqs. (6)–(8) and from the dispersion amplitudes via Eq. (9). The Lorentzian linewidths at [PDT]=0.1, 0.017, and 0.05 mM for hexane, decane, and hexadecane, respectively, were used to approximate the linewidth at zero spin exchange. Figure 2 shows typical values of ω_e derived from broadening and dispersion as functions of the PDT concentration. The slopes of linear least-squares fits constrained to the origin yield $K_e=(1.16\pm0.004)\times10^{10}\ \mathrm{s}^{-1}\,\mathrm{M}^{-1}$ and $(1.21\pm0.003)\times10^{10}\ \mathrm{s}^{-1}\,\mathrm{M}^{-1}$, respectively. Because spin-exchange-induced dispersion does not include any contribution from dipolar coupling, the near equality of the two rate constants shows that, without appreciable loss of accuracy, the broadening may be treated as resulting entirely from spin exchange. At the lowest temperatures in this study, we find that the slope of ω_e versus [PDT] derived from the broadening is slightly larger than that derived from the dispersion. The maximum difference reaches 6% in hexane at −60 °C and in decane at −20 °C. This shows that dipolar coupling likely does not contribute more than 6% to the broadening of the EPR lines, a discrepancy that contributes negligibly to results

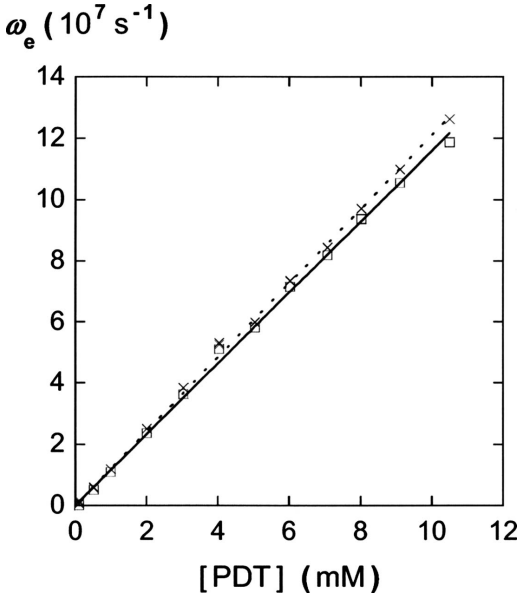

FIG. 2. Spin-exchange frequency determined from line broadening (□) and from dispersion (×) as a function of probe concentration in hexane at a temperature of 303 K. The solid and dashed lines are fitted through the origin.

reported herein. The broadening-derived and dispersion-derived frequencies have been averaged together in computing spin-exchange rate constants.

The coefficient κ for each temperature was obtained by fitting Eq. (10b) to the measured line broadenings and hyperfine spacings. Generally these fits were excellent, as shown for typical results in Fig. 3. The re-encounter time for that temperature was then calculated using Eq. (11).

Using literature viscosity data,[41,42] we present in Figs. 4 and 5 plots of τ_{RE}^{-1} and K_e vs T/η for all three solvents together with the hydrodynamic predictions, Eqs. (14b) and (13), respectively. It can be observed in Fig. 4 that the re-encounter rate τ_{RE}^{-1} in hexane is reasonably described by the hydrodynamic prediction at lower temperatures. This is not surprising since the van der Waals radius of hexane (3.0 Å) is smaller than that of PDT (3.5 Å). However, at higher temperatures for hexane and all temperatures for decane and hexadecane, the rate of re-encounters exceeds the hydrodynamic prediction. As expected, the order of departure from the hydrodynamic limit increases with greater solvent molecular volume. Figure 5 shows that the spin-exchange rate constant exceeds the hydrodynamic prediction at lower temperatures. However, the data from all three solvents fall on a common curve, demonstrating that the details of solvent are

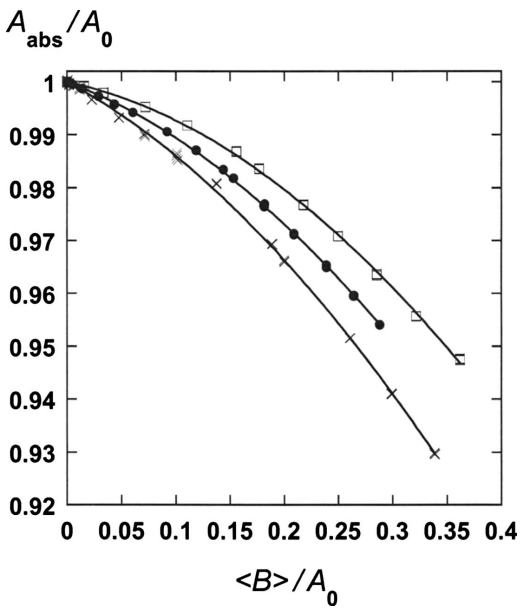

FIG. 3. Hyperfine spacing vs average line broadening (normalized with respect to hyperfine spacing at zero spin exchange) for hexane (□), decane (●), and hexadecane (×) at a temperature of 303 K. The curves are fits of the form of Eq. (10b) with R factors of 0.9997, 0.999 89, and 0.999 64 for hexane, decane, and hexadecane, respectively.

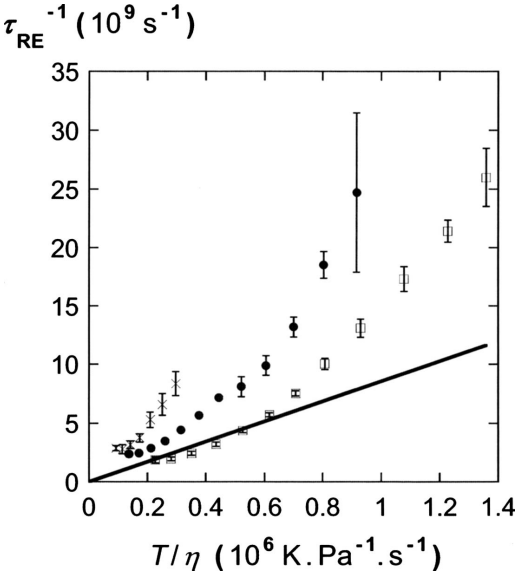

FIG. 4. Re-encounter collision rate vs T/η for hexane (□), decane (●), and hexadecane (×). The solid line is the Stokes–Einstein prediction.

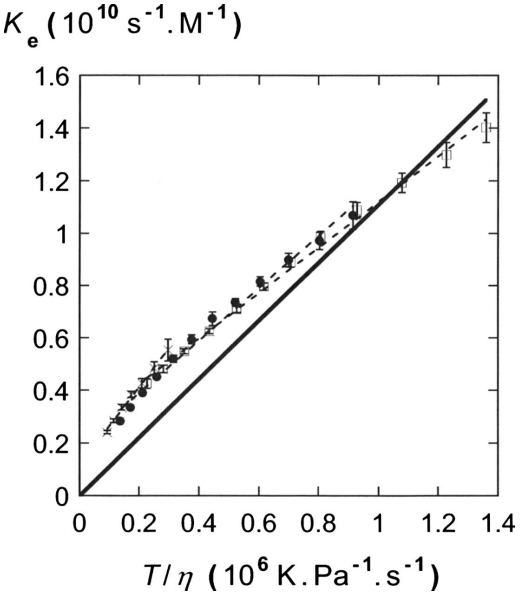

FIG. 5. Spin-exchange rate vs T/η for hexane (□), decane (●), and hexadecane (×). The dashed curves are linear fits, and the solid line is the Stokes–Einstein prediction.

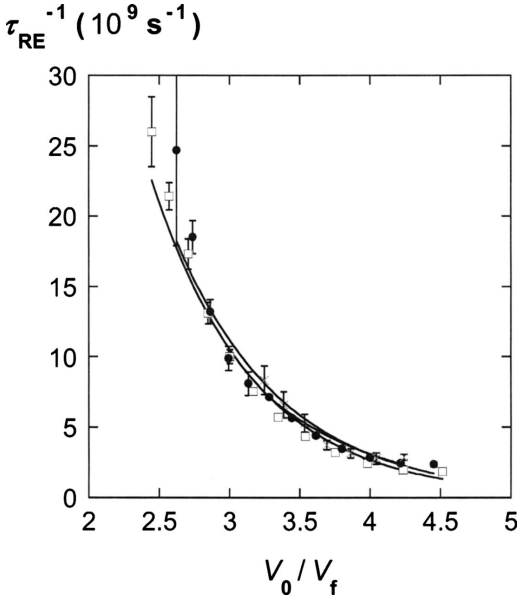

FIG. 6. Re-encounter collision rate vs reciprocal Doolittle relative free volume for hexane (□) decane (●), and hexadecane (×). The curves are fits to Eq. (17).

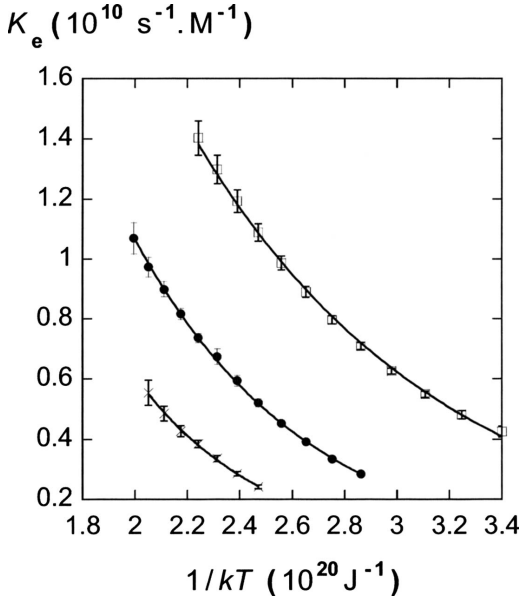

FIG. 8. Spin-exchange rate vs $1/kT$ for hexane (□), decane (●), and hexadecane (×). The curves are fits to Eq. (18) with R factors of 0.9995, 0.999 73, and 0.999 17 for hexane, decane, and hexadecane, respectively.

relatively unimportant determinants of the encounter rate constant. The re-encounter rate, on the other hand, is profoundly affected by the solvent details (Fig. 4).

To cast light upon the data in terms of local solvent properties as exemplified by the free volume, Figs. 6 and 7 show τ_{RE}^{-1} and K_e, respectively, as functions of V_0/V_f calculated from Doolittle's[37] empirical formulation. The re-encounters are largely determined by the free volume, forming a common curve in Fig. 6 for all three solvents, while the encounters do not. In Figs. 6 and 7 we also present the fits of the data to equations of the form of Eq. (17). As can be seen, the re-encounter and encounter rates fit this exponential form

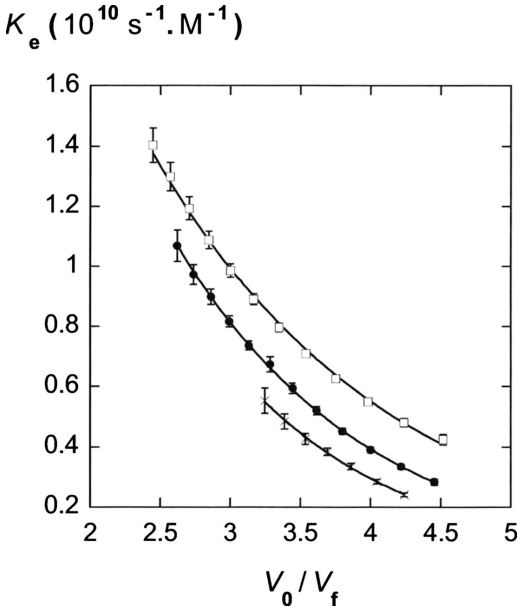

FIG. 7. Spin-exchange rate vs reciprocal Doolittle relative free volume for hexane (□), decane (●), and hexadecane (×). The curves are fits to Eq. (17).

very well. The values of the Doolittle–Cohen–Turnbull fit parameters B, denoted as B_{RE} and B_E as derived from re-encounters and encounters, respectively, are given in Table I.

According to Molin *et al.*,[4] one of the experimental methods of separating the strong from the weak exchange is based on plotting the K_e dependence on the temperature. For a strong exchange, K_e is expected to have an Arrhenius dependence upon temperature according to

$$K_e = K_{e0}e^{-A/kT}, \tag{18}$$

with A and K_{e0} constant. The fact that the values of K_e for all three solvents can be fitted very well to Eq. (18), as in Fig. 8, implies that the spin-exchange rate constant corresponds to a strong spin exchange. More generally, as K_e is directly proportional to the diffusion coefficient, Fig. 8 also shows evidence of Arrhenius behavior for the encounter diffusion of PDT in these solvents.

V. DISCUSSION

We have interpreted the additional line shift in Eq. (10b) compared with Eq. (10a) to be due to re-encounter spin-exchange events as previously proposed.[22] The additional shift arises from spin precession during the time intervals between re-encounters rather than during the collisions while the spin-exchange interaction is in effect.[31] Previous support for this proposal stemmed from three facts: (1) the magnitude of τ_{RE} was near that predicted by the SE equation for 16-doxylstearic acid methyl ester (16DSE) in ethanol and for 1-*H*-imidazol-1-yloxy-4,5-dihydro-4,4,5,5-tetramethyl-2-(*o*-nitrophenyl)-3-oxide in water (NN-NP),[22] (2) the relative spacings in the five-line spectrum of NN-NP were consistent with the prediction of the equations analogous to Eq. (11),[22] and (3) the values of τ_{RE} measured from both ^{15}N-PDT and ^{14}N-PDT nitroxides are the same.[43] See Figs. 8 and 9 of Ref. 22. Values of τ_{RE} at the same value of T/η were different for

NN-NP and 16DSE, but both the spin probe and the solvent were different. In this present work, the results in Fig. 4 provide further support for our interpretation where values of τ_{RE} are near those predicted by Eq. (14b). Here we have the advantage of avoiding the associative liquids of previous work,[21,22] employing the same spin probe and systematically varying the size of the alkane solvent. Therefore differences in the values of τ_{RE} at the same value of T/η may be attributed to differences in the solvent structure, as we expected when designing these experiments.

Turning to the encounter collision rate constant, one might have anticipated similar discrepancies with respect to the hydrodynamic picture that occur for re-encounters; however, Fig. 5 shows that this is not the case. The behavior of K_e depicted in Fig. 5, at first sight, seems to support a hydrodynamic description of the rate constant of encounters and furthermore seems to rule out any microscopic effects because there is no dependence on the relative sizes of the probe and solvent molecules. It is well known[44] that the SE equation provides a rather accurate description of experimental translational diffusion coefficients of small molecules even at high solvent densities.[44–49] The same is true for computer simulations employing hard spheres[50] and more complicated interactions.[51,52] Nevertheless, it can be argued that such systems are not intrinsically hydrodynamic in behavior and that the appearance of such behavior is an accidental result of canceling terms within a generalized diffusion coefficient.

Theoretical insight into the effect of microscopic interactions on diffusion was provided by Hynes *et al.*,[45] who showed that the usual hydrodynamic boundary condition on the relative velocity between the probe and solvent molecules at the moment of contact cannot hold microscopically. Their work has shown that in the case of low-density fluids with equally sized probe and solvent molecules, coupling molecular motion within an inner microscopic region to the motion of an outer hydrodynamic solvent region can lead to long-distance diffusion that accidentally mimics hydrodynamic behavior in the manner that our systems do. The momentum-conservation boundary condition proposed by Hynes *et al.*[45] is of the form

$$\hat{\mathbf{r}} \cdot \bar{\bar{\Pi}}_h(\hat{\mathbf{r}}\sigma) \cdot \hat{\mathbf{r}} = \hat{\mathbf{r}} \cdot \bar{\mathbf{F}}_m(\hat{\mathbf{r}}\sigma), \tag{19}$$

with σ as the radius of an imaginary spherical boundary between the microscopic and hydrodynamic regions, $\hat{\mathbf{r}}$ the unit vector radial to the boundary surface, $\bar{\bar{\Pi}}_h(\hat{\mathbf{r}}\sigma)$ the average hydrodynamic stress tensor, and $\bar{\mathbf{F}}_m(\hat{\mathbf{r}}\sigma)$ the microscopic collision force per area. The right-hand side of Eq. (19) allows microscopic details to enter via the Enskog friction constant. The diffusion coefficient is taken[45] to be the linear sum of an Enskog component D_{En} and a hydrodynamic component D_h such that

$$D = D_{En} + D_h. \tag{20}$$

When σ is taken to be the sum of the probe and solvent radii, the hydrodynamic contribution is found to be

$$D_h = \frac{kT}{4\pi(a + a_s)\eta}. \tag{21a}$$

Expressed in terms of the SE diffusion, the hydrodynamic component may be written as

$$D_h = \left(\frac{\mu}{1+\mu}\right) D_{SE}, \tag{21b}$$

with the SE prediction D_{SE} corrected by a factor accounting for the finite probe-to-solvent size ratio. The generalized hydrodynamic diffusion coefficient D_h replaces Eq. (12). Formally, Eqs. (21a) and (21b) are the Stokes–Einstein diffusion of the probe carrying a solvent molecule with it.

Compared to Eq. (12), the Enskog contribution in Eq. (20) increases D, while the size-corrected hydrodynamic contribution decreases it. For the low-density regime described by Hynes *et al.*[45] with $\mu=1$, D_{En} increases and D_h decreases with decreasing μ, leading to a partial cancellation of the Enskog and size-correction effects in Eq. (20). This leaves a diffusion value that is very close to D_{SE}. As μ decreases toward unity in a low-density fluid, the hydrodynamic term decreases while the Enskog term increases such that the diffusion coefficient departs from the prediction of Eq. (12) by only 21% even though the Enskog contribution dominates (see Fig. 1 and Table I of Ref. 45). Therefore, a common T/η curve for K_e in a low-density fluid would be explained as resulting from near cancellations of Enskog and size-correction terms, giving rise to a numerical semblance of hydrodynamic behavior. It is evident in Fig. 5 that in our systems an analogous, although perhaps not identical, cancellation takes place, giving rise to the semblance of hydrodynamic behavior in K_e.

The framework of Hynes *et al.*[45] serves as a useful backdrop against which to commence an understanding of the phenomenon. The degree of applicability of Eqs. (19), (20), (21a), and (21b) to our alkane-PDT systems is not precisely known at this stage. Our systems are similar in one respect to the regime described by that model in that our probe and solvent molecules are of comparable size; μ is close to unity. However, Hynes *et al.*[45] indicated that their theory was incomplete for a high-density system with μ close to unity, which is the regime in which we work. Another important difference is that their model pertains to systems that do not experience re-encounters, as the short-distance diffusion of their model does not admit backscattering. The boundary condition [Eq. (19)] entails a continuous, steady-state momentum transfer at the boundary between the inner microscopic region and the outer hydrodynamic region and therefore does not allow for the density fluctuations required to precipitate caging effects. It appears likely that in the systems of the present study, Enskog and size-correction effects also contribute to cancellations leading to the behavior observed in Fig. 5, but whether those terms alone account for the cancellation or whether other terms are also involved remains to be uncovered.

Let us now return to the experimental results for re-encounters in Fig. 4, where the existence of distinct curves reveals a clear dependence on the relative size of probe and solvent. Those data may be understood by the tentative pro-

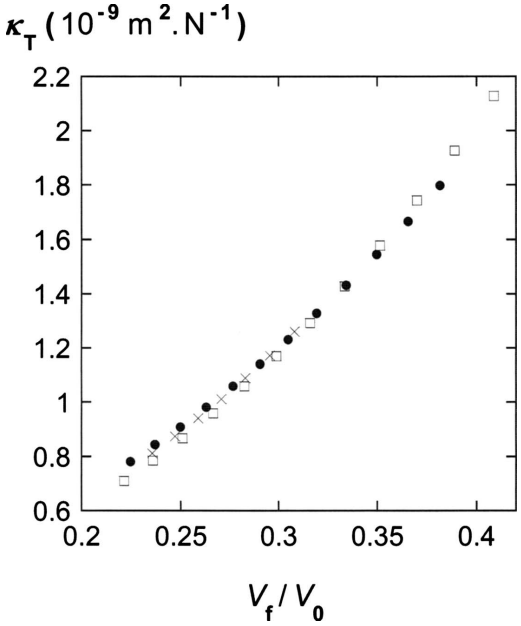

FIG. 9. Isothermal compressibility vs Doolittle relative free volume for hexane (□), decane (●), and hexadecane (×).

posal that because of the local density fluctuations required to precipitate caging effects, the motion of a probe during a re-encounter is less coupled to the outer hydrodynamic region than it is during steady-state microscopic diffusion. The resultant breakdown of the boundary condition [Eq. (19)] likely results in a predominant role of an Enskog term, which increases as μ decreases. This would lead to diffusion coefficients that increase beyond the Stokes–Einstein prediction of Eq. (12) as the solvent is changed from hexane to hexadecane. Because the Enskog diffusion coefficient increases with temperature,[45] the departures from Eq. (12) would also increase with temperature. Both of these effects are observed in Fig. 4. We do not wish to overinterpret the results in Fig. 4 until more solvents have been studied and a more accurate boundary condition is found. Nevertheless, it does seem clear that the prospects of studying details of bimolecular collisions in liquids are enhanced because of the access to re-encounter times. A distinct advantage to the spin-exchange approach is its ability to study both encounters and re-encounters, as well as rotational diffusion, within the same experiment.

The departures from the simple hydrodynamic formulation in the case of the well studied rotational diffusion are rather dramatic and have spurred extensive efforts[53–56] to improve the theoretical predictions. Hynes *et al.*[57] showed that the volume ratio of probe to solvent must be at least of order 100 (μ=4.6) for classical hydrodynamic equations to hold in rotational diffusion. Thus, it was expected that the SE equation would predict values of τ_{RE}^{-1} for PDT in hexane better than in the larger alkanes, and that is what we observe in Fig. 4. It is interesting that in re-encounter translational diffusion, the solvent volume need not be as much as an order of magnitude smaller than the probe volume for the SE approximation to have appreciable validity. This discrepancy between rotational and translational diffusion can be explained by the fact that in re-encounter translational diffusion, head-on collisions occur between probe molecules, as well as between probe and surrounding solvent molecules. Thus, the re-encounter time can be seen as a measure of linear momentum transfer, while the rotational correlation time can be seen as a measure of angular momentum transfer.[58] Since the transfer of linear momentum in re-encounter translational diffusion is greater than the transfer of angular momentum in rotational diffusion for the case of spherical molecules, it is not surprising that the departures from the simple hydrodynamic formulation in re-encounter diffusion occur at much lower values of the volume ratio of probe to solvent than those in rotational diffusion.

Figure 6 demonstrates that the re-encounter rate is well correlated to the free volume and fits the Doolittle–Cohen–Turnbull free volume equation [Eq. (17)][37–39] reasonably well. While the encounter rate constant for a given solvent fits well to Eq. (17), this equation does not predict its value in all three solvents. To our knowledge, there is no theory that predicts the effect of free volume on the re-encounter time. We have considered well known modifications to hydrodynamic theories for rotational correlation times such as those due to Dote *et al.*[53,54] and Kowert *et al.*[56] In the former, known as the quasihydrodynamic model, a correction factor accounting for free volume is applied to hydrodynamic predictions of rotational correlation times. In the proposal of Kowert *et al.*,[56] a factor entailing the probe and solvent radii is used to correct the hydrodynamic radius. We have attempted to apply correction factors from these theories to Eq. (14b) for re-encounter time. However, while these modifications improve the agreement for decane and hexadecane, they do not work well for hexane, the solvent for which the best agreement is expected.

Free volume is manifested macroscopically as the isothermal compressibility κ_T defined as

$$\kappa_T = -\frac{1}{V}\left(\frac{\partial V}{\partial P}\right)_T. \tag{22}$$

Figure 9, prepared with literature data,[59–70] shows that κ_T is highly correlated with the Doolittle relative free volume for the three alkanes in this study.

A particularly intriguing and promising result of the study is what appears to be a common curve when the re-encounter time is plotted against the isothermal compressibility for all three solvents, as shown in Fig. 10. The compressibilities in Figs. 9 and 10 for the measurement temperatures are based on exponential curve fits generated from literature compressibility data[59–70] at various temperatures. In the case of hexane, no compressibility data were found in the literature for temperatures below 273 K, which is the range in which half of the spectra for this solvent were taken. An exponential curve with respect to temperature for experimental compressibilities starting at 273 K was found to be the best fit for these data, and this was extrapolated to the lower temperatures. To verify the accuracy of the extrapolation, the literature compressibilities for hexane were plotted against literature density data,[71–75] which included densities at T below 273 K, and an exponential curve was found to fit best the relation between compressibility and density. As the density ρ exhibits a linear dependence on

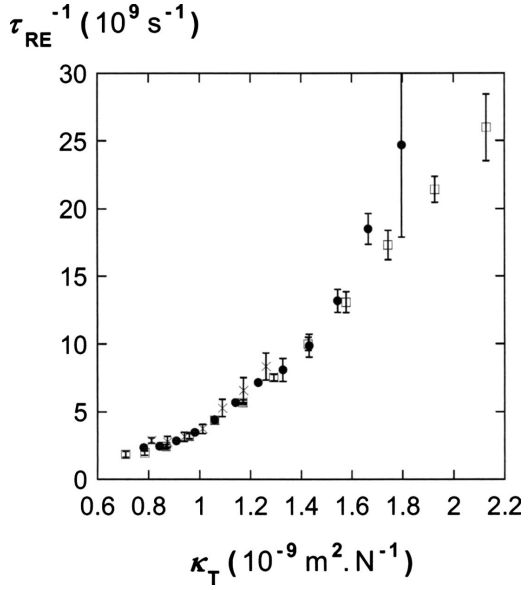

FIG. 10. Re-encounter collision rate vs isothermal compressibility for hexane (□), decane (●), and hexadecane (×).

temperature, a successful exponential fit for κ_T vs ρ would imply the same fit for κ_T vs T. The values for κ_T obtained from the exponential fit with respect to ρ were then fitted to the corresponding temperatures and were indeed found to fit them exponentially. The values for the compressibility at $T<273$ obtained from fitting to the density data were found to be in excellent agreement with those resulting from the fit of the compressibility data directly to temperature. Reasonable confidence can therefore be placed in the compressibilities computed from curve fitting. A plot of K_e vs κ_T (not shown) shows three distinct nearly linear curves similar to those in Fig. 7.

The prospect of a universal curve as that in Fig. 10 for all alkanes means that measurement of the probe re-encounter rate may be a useful method to determine indirectly the isothermal compressibility of a substance through EPR.

VI. CONCLUSION

Spin-exchange measurements of PDT in three alkanes support a previous hypothesis that the line shift linear in ω_e is due to spin precession between re-encounters as follows: (1) the order of magnitude of the values of τ_{RE} is in agreement with the SE equation and (2) departures from the SE equation are in the direction expected from the Enskog microscopic contributions to the diffusion coefficient. Values of τ_{RE} may be measured with good precision by employing nonlinear fitting techniques to analyze EPR spectra under conditions of Heisenberg spin exchange. The solvent dependence of τ_{RE} is well correlated with the isothermal compressibility, which is in turn correlated with the free volume within the liquid. In contrast, the encounter rate constant does not depend on the solvent, following an apparent SE behavior; however, it is likely that this behavior is due, in part, to near cancellation of terms within a generalized diffusion coefficient.

ACKNOWLEDGMENTS

The authors gratefully acknowledge support from NIH Grant Nos. 5 S06 GM48680-09 (B.L.B.), 3 S06 GM48680-10S1 (M.R.K. and M.P.), and 2 S06 GM48680-12A1 (M.P.).

[1] D. Kivelson, J. Chem. Phys. **33**, 1094 (1960).
[2] J. H. Freed, J. Chem. Phys. **45**, 3452 (1966).
[3] M. T. Jones, J. Chem. Phys. **38**, 2892 (1963).
[4] Y. N. Molin, K. M. Salikhov, and K. I. Zamaraev, *Spin Exchange. Principles and Applications in Chemistry and Biology*, Springer Series in Chemical Physics Vol. 8 (Springer-Verlag, New York, 1980).
[5] K. M. Salikhov, A. B. Doctorov, Y. N. Molin, and K. I. Zamaraev, J. Magn. Reson. (1969-1992) **5**, 189 (1971).
[6] J. D. Currin, Phys. Rev. **126**, 1995 (1962).
[7] Y. Ayant, R. Besson, and A. Salvi, J. Phys. (Paris) **36**, 571 (1975).
[8] C. S. Johnson, Jr., Mol. Phys. **12**, 25 (1967).
[9] A. E. Stillman, L. J. Schwartz, and J. H. Freed, J. Chem. Phys. **73**, 3502 (1980).
[10] B. Berner and D. Kivelson, J. Phys. Chem. **83**, 1406 (1979).
[11] A. L. Kovarskii, A. M. Wasserman, and A. L. Buchachenko, J. Magn. Reson. (1969-1992) **7**, 225 (1972).
[12] M. P. Eastman, R. G. Kooser, M. R. Das, and J. H. Freed, J. Phys. Chem. **71**, 38 (1969).
[13] M. P. Eastman, G. V. Bruno, and J. H. Freed, J. Chem. Phys. **52**, 2511 (1970).
[14] M. D. King, J. H. Sachse, and D. Marsh, J. Magn. Reson. (1969-1992) **72**, 257 (1987).
[15] J. H. Sachse, M. D. King, and D. Marsh, J. Magn. Reson. (1969-1992) **71**, 385 (1987).
[16] G. Martini and M. Bindi, J. Colloid Interface Sci. **108**, 133 (1985).
[17] T. A. Miller, R. N. Adams, and P. M. Richards, J. Chem. Phys. **44**, 4022 (1966).
[18] A. Nayeem, S. B. Rananavare, V. S. S. Sastry, and J. H. Freed, J. Chem. Phys. **91**, 6887 (1989).
[19] W. Plachy and D. Kivelson, J. Chem. Phys. **47**, 3312 (1967).
[20] B. L. Bales and M. Peric, J. Phys. Chem. B **101**, 8707 (1997).
[21] B. L. Bales and M. Peric, J. Phys. Chem. A **106**, 4846 (2002).
[22] B. L. Bales, M. Peric, and I. Dragutan, J. Phys. Chem. A **107**, 9086 (2003).
[23] I. N. Levine, *Physical Chemistry*, 4th ed. (McGraw-Hill, New York, 1995).
[24] R. M. Noyes, J. Chem. Phys. **22**, 1349 (1954).
[25] F. C. Collins and G. E. Kimball, J. Colloid Sci. **4**, 425 (1949).
[26] A. J. Benesi, J. Phys. Chem. **86**, 4926 (1982).
[27] B. A. Kowert, N. C. Dang, K. T. Sobush, and L. G. Seele III, J. Phys. Chem. A **105**, 1232 (2001).
[28] B. H. Robinson, C. Mailer, and A. W. Reese, J. Magn. Reson. **138**, 210 (1999).
[29] B. H. Robinson, C. Mailer, and A. W. Reese, J. Magn. Reson. **138**, 199 (1999).
[30] B. L. Bales, in *Biological Magnetic Resonance*, edited by L. J. Berliner and J. Reuben (Plenum, New York, 1989), Vol. 8, p. 77.
[31] K. M. Salikhov, J. Magn. Reson. (1969-1992) **63**, 271 (1985).
[32] See EPAPS Document No. E-JCPSA6-129-619830 for an explanation of the derivation. For more information on EPAPS, see http://www.aip.org/pubservs/epaps.html.
[33] Y. H. Zhao, M. H. Abraham, and A. M. Zissimos, J. Org. Chem. **68**, 7368 (2003).
[34] A. Bondi, J. Phys. Chem. **68**, 441 (1964).
[35] L. L. Jones and R. N. Schwartz, Mol. Phys. **43**, 527 (1981).
[36] J. Frenkel, *Kinetic Theory of Liquids* (Dover, New York, 1955).
[37] A. K. Doolittle, J. Appl. Phys. **22**, 1471 (1951).
[38] M. H. Cohen and D. Turnbull, J. Chem. Phys. **31**, 1164 (1959).
[39] B. A. Kowert, N. C. Dang, K. T. Sobush, and L. G. Seele III, J. Phys. Chem. A **104**, 8823 (2000).
[40] J. S. Hyde and W. K. Subczynski, in *Biological Magnetic Resonance*, edited by L. J. Berliner and J. Reuben (Plenum, New York, 1989), Vol. 8, p. 399.
[41] B. Ancian, B. Tiffon, and J. E. Dubois, J. Chem. Phys. **74**, 5857 (1981).
[42] D. S. Viswanath and G. Natarajan, *Data Book on the Viscosity of Liquids* (Hemisphere, New York, 1989).
[43] B. L. Bales, M. Meyer, S. Smith, and M. Peric, J. Phys. Chem. A **112**, 2177 (2008).

[44] J. T. Hynes, Annu. Rev. Phys. Chem. **28**, 301 (1977).
[45] J. T. Hynes, R. Kapral, and M. Weinberg, J. Chem. Phys. **70**, 1456 (1979).
[46] E. McLaughlin, Trans. Faraday Soc. **55**, 28 (1959).
[47] C. R. Wilke, Chem. Eng. Prog. **45**, 218 (1949).
[48] J. T. Edward, J. Chem. Educ. **47**, 261 (1970).
[49] M. McCool and L. A. Woolf, J. Chem. Soc., Faraday Trans. 1 **68**, 1971 (1972).
[50] B. J. Alder, D. M. Gass, and T. E. Wainwright, J. Chem. Phys. **53**, 3813 (1970).
[51] W. E. Alley and B. J. Alder, J. Chem. Phys. **63**, 3764 (1975).
[52] E. M. Gosling, I. R. McDonald, and K. Singer, Mol. Phys. **26**, 1475 (1973).
[53] J. L. Dote, D. Kivelson, and R. N. Schwartz, J. Phys. Chem. **85**, 2169 (1981).
[54] J. L. Dote and R. N. Schwartz, J. Phys. Chem. **85**, 3756 (1981).
[55] M. Roy and S. Doraiswamy, J. Chem. Phys. **98**, 3213 (1993).
[56] B. A. Kowert, K. T. Sobush, C. F. Fuqua, C. L. Mapes, J. B. Jones, and J. A. Zahm, J. Phys. Chem. A **107**, 4790 (2003).
[57] J. T. Hynes, R. Kapral, and M. Weinberg, J. Chem. Phys. **67**, 3256 (1977).
[58] I. Artaki and J. Jonas, J. Chem. Phys. **82**, 3360 (1985).
[59] D. V. Matyushov and R. Schmid, Ber. Bunsenges. Phys. Chem. **98**, 1590 (1994).
[60] W. K. Tolley, R. M. Izatt, and J. L. Oscarson, Thermochim. Acta **181**, 127 (1991).
[61] K. Malakondaiah, K. Subbarangaiah, and S. V. Subrahmanyam, Phys. Chem. Liq. **23**, 49 (1991).
[62] A. Chandrasekhar, K. N. Surendranath, and A. Krishnaiah, Acta Chim. Hung. **127**, 345 (1990).
[63] E. Aicart, G. Tardajos, and M. Diaz Pena, J. Chem. Eng. Data **25**, 140 (1980).
[64] M. Diaz Pena, G. Tardajos, C. Menduina, and R. L. Arenosa, J. Chem. Thermodyn. **11**, 67 (1979).
[65] A. Blinovska and W. Brostow, J. Chem. Thermodyn. **7**, 787 (1975).
[66] V. N. Kartsev, Zh. Fiz. Khim. **50**, 764 (1976).
[67] M. Diaz Pena and G. Tardajos, J. Chem. Thermodyn. **10**, 19 (1978).
[68] B. P. Sahli, H. Gager, and A. J. Richard, J. Chem. Thermodyn. **8**, 179 (1976).
[69] G. Hahn, K. Ulcay, P. Sverjda, and M. A. Siddiqi, J. Chem. Eng. Data **41**, 319 (1996).
[70] J. S. Chang, M. J. Lee, and H. M. Lin, J. Chem. Eng. Data **43**, 233 (1998).
[71] J. Troncoso, D. Bessieres, C. A. Cerdeirina, E. Carballo, and L. Romani, J. Chem. Eng. Data **49**, 923 (2004).
[72] T. Katayama and T. Nitta, J. Chem. Eng. Data **21**, 194 (1976).
[73] M. L. McGlashan and A. G. Williamson, J. Chem. Eng. Data **21**, 196 (1976).
[74] M. F. Bolotnikov, Y. A. Neruchev, Y. F. Melikhov, V. N. Verveyko, and M. V. Verveyko, J. Chem. Eng. Data **50**, 1095 (2005).
[75] A. J. Queimada, I. M. Marrucho, J. A. P. Coutinho, and E. H. Stenby, Paper Presented at the 15th Symposium on Thermophysical Properties, Boulder, Colorado, June 22–27, 2003 (unpublished).